Global Optimization of Deformable Surface Meshes Based on Genetic Algorithms

Jussi Tohka
Institute of Signal Processing
Tampere University of Technology
P.O.Box 553, FIN-33101, Tampere, Finland,
jussi.tohka@cs.tut.fi

Abstract

Deformable models are by their formulation able to solve surface extraction problem from noisy volumetric image data encountered commonly in medical image analysis. However, this ability is shadowed by the fact that the minimization problem formulated is difficult to solve globally. Constrained global solutions are needed, if the amount of noise is substantial. This paper presents a new optimization strategy for deformable surface meshes based on real coded genetic algorithms. Real coded genetic algorithms are favored over binary coded ones because they can more efficiently be adapted to the particular problem domain. The experiments with synthetic images are performed. These demonstrate that the applied deformable model is able extract a surface from a noisy volumetric image. Also superiority of the proposed approach compared to a greedy minimization with multiple initializations is demonstrated.

1. Introduction

Deformable surface models [8] are sophisticated approaches for surface extraction from volumetric image data. The problem is formulated as minimization of the energy of the surface. A surface has two energy functions associated with it. The external energy is derived from the image data and the internal energy derives from the shape of the surface. The total energy is a weighted sum of these two functions. By the internal energy these models are in principle able to cope with noise, outliers and missing data, problems often present in volumetric medical images. If the image has low signal to noise ratio the energy function of the deformable surface can have numerous local minima. Furthermore, it is often assumed that a good initial positioning for the target surface is available. However, automated initialization methods based on binarization such as in [2] may not perform well if the image data is noisy. Above considerations lead us to consider a global optimization framework for automated surface extraction with deformable models. Then, the energy of the deformable surface is globally minimized, possibly with constraints related to the size of the surface or its location in the image. Such a problem, even if properly formulated, is difficult to solve. In this paper a novel solution based on genetic algorithms to the optimization problem is proposed.

Genetic algorithms (GA) [5] have been successfully applied to the number of complex optimization problems. They are based on the genetic processes of biological organisms. Mimicking the natural selection and reproduction an initial population evolves to the solution of the problem at the hand. In the current study, a genetic algorithm is applied to globally minimize the energy of a deformable surface mesh. The minimum obtained is further strengthened by a greedy algorithm [9]. Then the resolution of the mesh is increased to correspond to that of the image. Finally, the energy of the fine mesh is locally minimized for the capture of details of the target surface. Throughout the paper it will be assumed that there is only a single closed surface homeomorphic to sphere in the image.

In [1] a GA is used for a resembling optimization task, namely to minimize the energy of the snake [7]. Besides that in [1] contours were considered, the GA applied there differed from the one we apply and also there the optimization was performed solely with the GA. Moreover, the internal energy of the snake is not scale invariant, what leads to biased results.

2. Deformable model

The applied deformable model is presented in this section. The model is based on a simplex mesh representation

of the surfaces [3]. The simplex mesh $\mathcal{M}$ consists of a set of discrete points, called mexels, $\mathbf{V} \subset \mathbb{R}^3$ and adjacency relations between mexels. Each mexel $\mathbf{v}_i \in \mathbf{V}$ is adjacent to exactly three other mexels $\mathbf{v}_{i_1}, \mathbf{v}_{i_2}, \mathbf{v}_{i_3}$, which are its neighbours. The neighbourhood relations can be modeled by a 3-regular simple graph, the graph of the mesh. Simplex meshes are topological duals of triangular meshes [3], and therefore one can generate simplex meshes from triangular ones as presented in detail in [10].

The key to surface extraction with deformable models is the definition of its energy function. With deformable meshes the energy of the mesh is the sum of energies of individual mexels. An alternative approach with deformable meshes is to consider forces acting on mexels. Our attention is directed to the energy-based approach due to the global optimization framework. The energy of the mesh is

$$\begin{aligned} E(\mathcal{M}) &= \lambda E_{int}(\mathcal{M}) + (1-\lambda) E_{ext}(\mathcal{M}) \qquad (1) \\ &= \sum_{i=1}^{|\mathbf{V}|} [\lambda E_{int}(\mathbf{v}_i) + (1-\lambda) E_{ext}(\mathbf{v}_i)], \end{aligned}$$

where E_{int} is the internal energy, E_{ext} is the external energy and $\lambda \in [0,1]$ is the regularization parameter. The internal energy is defined as

$$E_{int}(\mathbf{v}_i) = \frac{||\mathbf{v}_i - \frac{1}{3}\sum_{j=1}^{3} \mathbf{v}_{i_j}||^2}{A(\mathcal{M})}. \qquad (2)$$

The internal energy is similar in spirit with the surface orientation continuity constraint proposed in [3]. The area constant $A(\mathcal{M})$ is required for scale invariance of the internal energy. We calculate it as the average area of faces of the mesh $\mathcal{M}$. Areas of faces are calculated by triangulating them. With the area constant, the internal energy is scale, rotation and translation invariant. The external energy is defined as

$$E_{ext}(\mathbf{v}_i) = 1 - \frac{I(\mathbf{v}_i)^2}{\max_{\mathbf{x}\in\mathbb{R}^3} I(\mathbf{x})^2}, \qquad (3)$$

where $I(\mathbf{x})$ is the intensity of the input image. It is assumed that $I(\mathbf{x}) \geq 0$ for all $\mathbf{x} \in \mathbb{R}^3$. Constraints can be embedded in (2) by adding suitable penalty terms.

3. Surface extraction based on the deformable mesh and a genetic algorithm

In this section, an algorithm for the global surface extraction in noisy conditions is presented. First, we introduce a hybrid algorithm of a GA and the greedy algorithm [9] to minimize (2). Then, the applied GA is described with more detail because the novelty in the work lies there.

3.1. Hybrid algorithm for deformable mesh optimization

The optimization process is divided in four separate steps:

1. Global minimization of the energy of the mesh by a GA;
2. Greedy minimization of the energy of the mesh obtained from first step;
3. Adaptation of the resolution of the mesh;
4. Minimization of the energy of the adapted mesh for the final solution by the greedy algorithm;

Optimization is not solely done with GAs due to their slow convergence in the final stages of the minimization. The purpose of the GA is to perform an exploration for an approximative surface in the close vicinity of the real target. Thereafter a local search by the greedy algorithm will be more efficient (than the GA) for the surface extraction.

During the first two steps a coarse mesh, as compared to the resolution of the image, is applied in order to reduce the computational burden. The resolution of the mesh is then adapted to correspond to that of the image. The adaptation procedure is the following: If the area of a face of the mesh is greater than a given threshold, then the face is divided by applying T_2^2 operator defined in [3].

3.2. Genetic algorithm

The basic structure of a GA is presented in Algorithm 1.

Algorithm 1 Genetic Algorithm

$t \leftarrow 0$
initialize a population $P(t)$ of surface meshes
evaluate $P(t)$ by computing the energy of each individual in it
while NOT termination condition **do**
  $t \leftarrow t + 1$
  select $P(t)$ from $P(t-1)$
  recombine $P(t)$
  evaluate $P(t)$
end while

The populations consist of simplex meshes having the same graph. Instead of the traditional binary coding, the real coded GA (RCGA) is applied [6]. With RCGAs it is possible to define recombination operators that can do well in a particular problem domain. This is especially important with deformable meshes because meaningful but

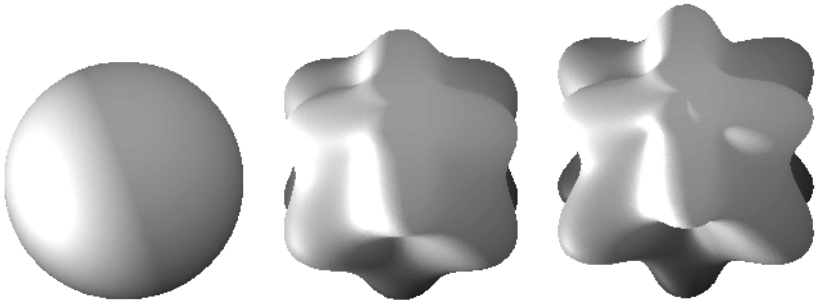

a) b) c)

Figure 1. Test surfaces: a) sphere b) metasphere 1 c) metasphere 2.

random initial populations are hard or even impossible to construct. The strategy used in this study was to begin with an initial population consisting only surface meshes of simple shapes and produce the randomness in shapes by applying suitable recombination operators. The initial population was constructed by transforming a sphere mesh of 320 mexels by random affine transformations. We applied BLX-α crossover [4, 6]: If $\mathbf{V}^1 = \{\mathbf{v}_1^1, \ldots, \mathbf{v}_N^1\}$ and $\mathbf{V}^2 = \{\mathbf{v}_1^2, \ldots, \mathbf{v}_N^2\}$ are the parents, then the offspring is $\mathbf{W}^j = \{\mathbf{w}_1^j, \ldots, \mathbf{w}_N^j\}, j = 1, 2$, where $\mathbf{w}_i^1 = \mathbf{v}_i^1 + r_i(\mathbf{v}_i^2 - \mathbf{v}_i^1)$, $\mathbf{w}_i^2 = \mathbf{v}_i^2 + r_i(\mathbf{v}_i^1 - \mathbf{v}_i^2)$ and each r_i is randomly chosen from the interval $[-\alpha, 1+\alpha]$. We did not apply any mutation due to the selected crossover operator.

The tournament selection with tournament size of ten was applied. The crossover rate was 1. From each generation, ten meshes of lowest energy automatically survived to the next generation.

4. Experiments and Results

A set of synthetic test images was used to test the introduced energy minimization method. The images contained a closed surface of intensity values of one. See Fig. 1 for surfaces, which are metaspheres introduced in [10]. Dimensions for the applied synthetic images were $64 \times 64 \times 64$. For each surface the image set contained a noiseless version and two noisy versions corrupted with white Gaussian noise. Variances of noise were 0.3 and 0.6. Noisy images were filtered with a Gaussian filter. The filter had $3 \times 3 \times 3$ kernel with the standard deviation equal to 1.

The population size for the GA was 4000. The regularization parameter $\lambda = 0.3$ in all tests. The threshold for the resolution adaptation routine was 3. The GA was terminated when 100 generations were evaluated. In all cases, after 100 generations, the speed of convergence was already very low. BLX-0.3 crossover was used. BLX-0.1 and BLX-0.5 crossovers were also tested, but they gave worse results than the selected crossover operator. With BLX-0.1, the problem was premature convergence. When BLX-0.5 operator was applied, the speed of convergence was too slow: In a few experiments that were made, even within 1000 generations no better solution than the best initial one was found.

Quantitative test results were computed with the following measure: Let $TRUE$ denote the set of voxels inside the true (digital) surface and let $EXTRACTED$ be the set of voxels inside the extracted surface. Then the error is

$$\epsilon = 1 - \frac{|EXTRACTED \cap TRUE|}{|EXTRACTED \cup TRUE|}. \qquad (4)$$

To depict the measure assume that the true surface is a sphere of radius 16 and the extracted surface is identical expect that it is translocated one unit in each direction from the true surface. Then $\epsilon = 0.16$.

Energies of meshes after the GA and the first greedy minimization (Step 2 in the hybrid algorithm) as well as values of ϵ after each minimization step are listed in Table 1. Some qualitative results are shown in Figs. 2 and 3. All surfaces were accurately extracted from noiseless images, as can be seen from Table 1. When the variance of noise was 0.3, sphere and metasphere 1 were extracted well as can be seen from Figs. 2 and 3. With metasphere 2, the result was not good in highly curved parts of the surface (See Fig. 2), but acceptable in a global sense. When the variance of noise was 0.6, sphere was extracted well. With metasphere 1, highly curved details of the surface were not captured, but overall result was still acceptable. The extraction result for metasphere 2 in this case was not good. Application of the greedy algorithm after the GA is justified since the energy of the mesh was lowered in each case. For noiseless images and the two metaspheres, the decrease was notable. However, in two cases where the surface in the image was sphere, values of ϵ were slightly higher after the first greedy minimization than after the GA. Indeed, there is no guarantee that a lower energy yields a better result. However, our global optimization strategy is still

valid, because we can assume that, on the average, energies are lower near the true surface. Therefore a low energy value yields a good result.

Also another simulation was made. In the simulation all meshes in the initial population for the GA were optimized by the greedy algorithm. The surface to be extracted was the sphere in a noisy image. When noise variance was 0.6 (respectively 0.3), the lowest energy after all minimizations was 0.1546 (0.1681). With the proposed hybrid algorithm a better result (after the first greedy minimization) 0.1372 (0.1599) was achieved. With the hybrid algorithm also lower errors ϵ were obtained. Minimization of energies of all the meshes with the greedy algorithm has a complexity about 16 times greater than 100 generations of the GA.

5. Discussion and Summary

We have shown how to apply genetic algorithms to optimization of deformable surface meshes. The proposed scheme is well-suited for noisy conditions. However, two points ought to be studied further. The initial population should contain more shapes than just ellipsoids to make the method more flexible for different shapes of the target surface. The crossover-operator applied is not optimal. A lot of the computation time is wasted by evaluating meshes that are of irregular shape and hence have high energy. However, all the other crossover operators tested performed worse than BLX-α operators. BLX-α crossovers also tend to produce non-smooth meshes that are easily corrected by the greedy algorithm, and therefore they are well-suited for simple hybrid algorithms like the one which we have presented.

The choice of value of α is a tradeoff between computation time and the goodness of the result. A good compromise is achieved by setting $\alpha = 0.3$. However, in some cases better optimization results may be achieved at the expense of longer computation time by increasing α.

To summarize, the global optimization of deformable meshes provides a sound framework for automated surface extraction from noisy images, a problem commonly encountered when processing medical images. In this paper, a novel technique for the global optimization of deformable surface meshes is proposed. The experiments suggest that with the global optimization scheme, surfaces can be extracted also from noisy images.

Acknowledgment

The author financially supported by *Tampere Graduate School of Information Science and Engineering*. This work was supported also by *Academy of Finland*.

References

[1] L. Ballerini. Genetic snakes for medical images segmentation. In *Mathematical Modeling and Estimation Techniques in Computer Vision,Proc. SPIE Vol. 3457*, 1998.

[2] H. Delingette. Initialization of deformable models from 3D data. In *Proceedings of the Sixth Int. Conf. on Computer Vision (ICCV'98)*, 1998.

[3] H. Delingette. General object reconstruction based on simplex meshes. *International Journal of Computer Vision*, 32:111–142, 1999.

[4] L. J. Eshelman and J. D. Schaffer. Real-coded genetic algorithms and interval schemata. In *Foundations of Genetic Algorithms 2*. Morgan Kaufmann Publishers, 1993.

[5] D. Goldberg. *Genetic Algorithms in Search, Optimization and Machine Learning*. Addison-Wesley, 1989.

[6] F. Herrera, M. Lonzano, and J. L. Verdegay. Tackling real-coded genetic algorithms: Operators and tools for behaviorial analysis. *Artificial Intelligence Review*, 12(4), 1998.

[7] M. Kass, A. Witkin, and D. Terzopoulos. Snakes: Active contour models. *International Journal of Computer Vision*, 1(4):321 – 331, 1988.

[8] D. Terzopoulos, A. Witkin, and M. Kass. Constraints on deformable models: Recovering 3D shape and nonrigid motion. *Artificial Intelligence*, 36:91 – 123, 1988.

[9] D. Williams and M. Shah. A fast algorithm for active contours and curvature estimation. *CVGIP: Image Understanding*, 55(1):14 – 26, 1992.

[10] C. Xu. *Deformable Models with Application to Human Celebral Cortex Reconstruction from Magnetic Resonance Images*. PhD thesis, the Johns Hopkins University, 1999.

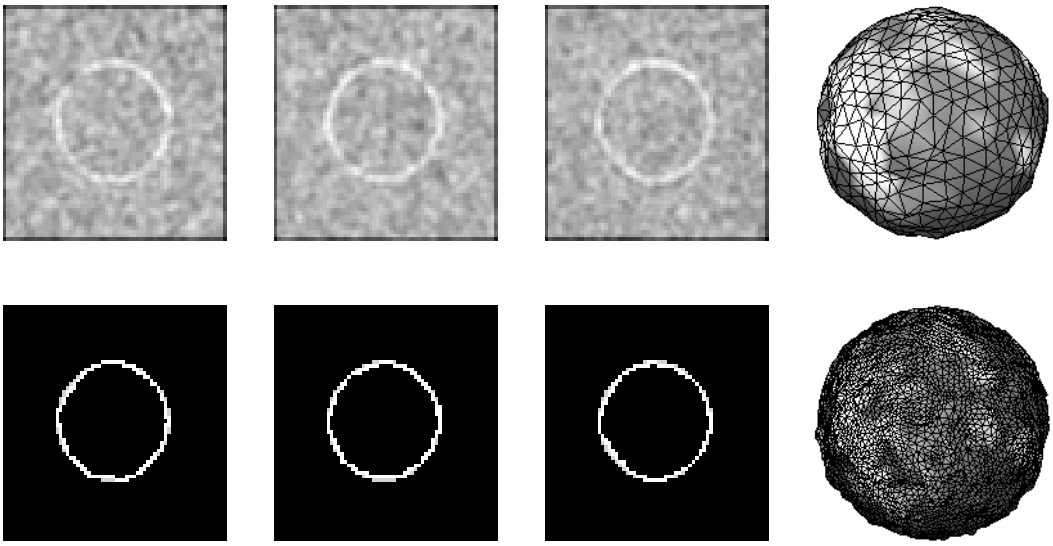

a) b) c) d)

Figure 2. The extracted sphere from the image with noise of the variance 0.3. Columns a), b) and c). Top row : central cross sections of the filtered noisy image in (resp.) xy, xz and yz-planes. Bottom row: central cross sections of the extracted surface (in white) and the true surface (in grey) in (resp.) xy, xz and yz planes. The column d). The extracted meshes after the 1st greedy (on top) and after the 2nd greedy minimization (on bottom). Simplex meshes have been triangulated before visualization.

Table 1. Energies and values of the error criteria (4) of meshes after the minimization steps. Symbol σ^2 denotes the variance of noise in the image. For target surfaces see Fig. 1. Energies after the 1st greedy minimization and the 2nd greedy minimization are not comparable because meshes after the 2nd greedy minimization have more mexels. Therefore energy values after the 2nd greedy minimization are omitted from the table.

		energy of the mesh after		error after		
surface	σ^2	GA	1st greedy	GA	1st greedy	2nd greedy
sphere	0	0.0113	0.0038	0.05	0.09	0.04
metasphere 1	0	0.0745	0.0069	0.12	0.11	0.04
metasphere 2	0	0.1643	0.0107	0.27	0.17	0.07
sphere	0.3	0.1768	0.1599	0.09	0.08	0.07
metasphere 1	0.3	0.1742	0.1365	0.16	0.11	0.08
metasphere 2	0.3	0.2076	0.1739	0.26	0.21	0.18
sphere	0.6	0.1518	0.1372	0.08	0.11	0.10
metasphere 1	0.6	0.2036	0.1646	0.27	0.18	0.18
metasphere 2	0.6	0.2004	0.1695	0.39	0.36	0.35

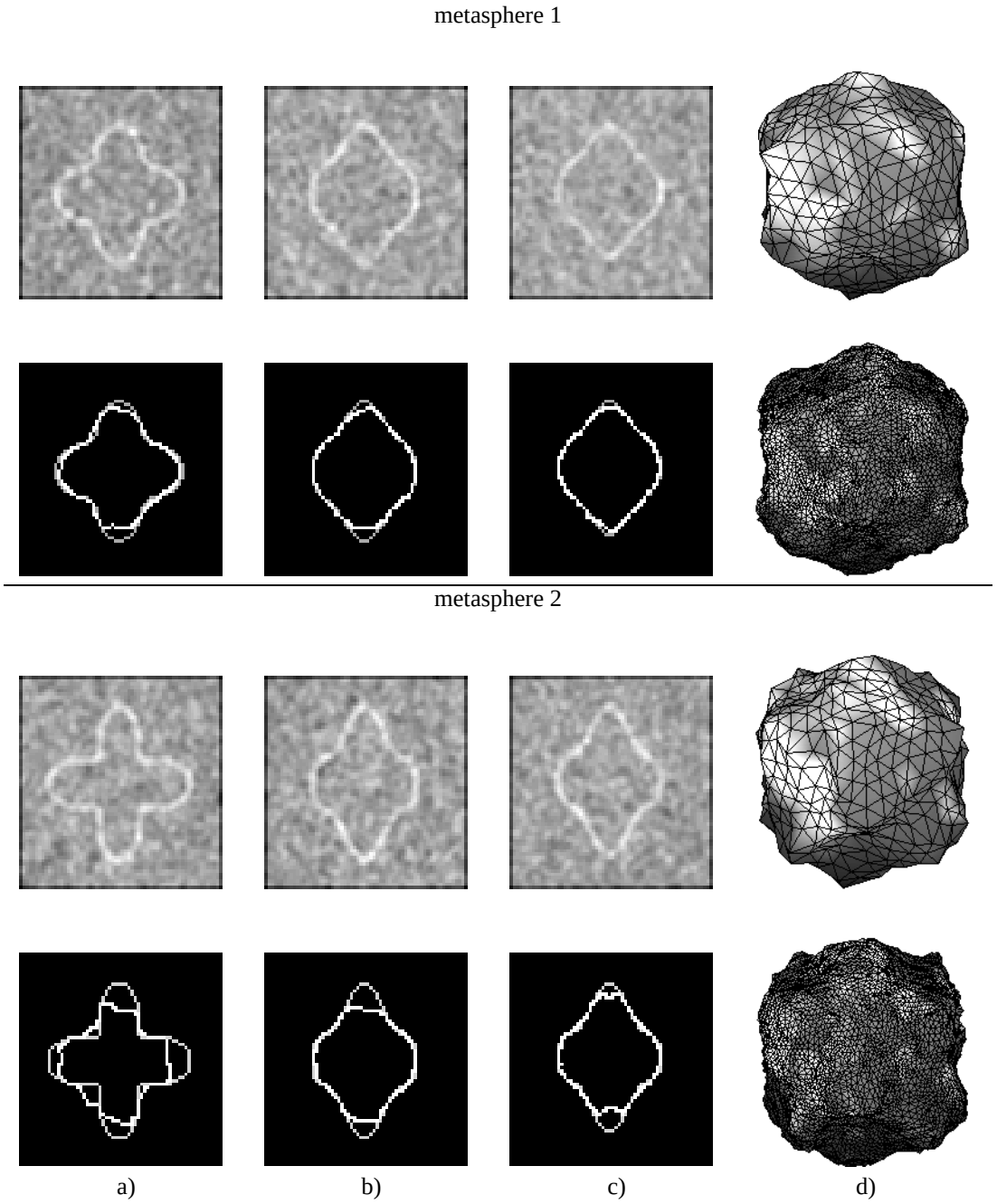

Figure 3. The extracted metasphere 1 and metasphere 2 from the images with noise of the variance 0.3. Two topmost rows are dedicated to metasphere 1 and two bottom rows deal with metasphere 2. Columns a), b) and c). Top row for both surfaces : central cross sections of the filtered noisy image in (resp.) xy, xz and yz-planes. Bottom row for both surfaces: central cross sections of the extracted surface (in white) and the true surface (in grey) in (resp.) xy, xz and yz planes. The column d). The extracted meshes after the 1st greedy (on top) and after the 2nd greedy minimization (on bottom). Simplex meshes have been triangulated before visualization.